Optical Pulling and Pushing Forces in Bilayer $\mathcal{PT}$-Symmetric Structures

Rasoul Alaee,[1,*] Johan Christensen,[2] and Muamer Kadic[3]

[1] *Max Planck Institute for the Science of Light, Erlangen 91058, Germany*
[2] *Instituto Gregorio Millan Barbany, Universidad Carlos III de Madrid, ES-28916 Leganés, Madrid, Spain*
[3] *Institut FEMTO-ST, UMR 6174, CNRS, Université de Bourgogne Franche-Comté, 25000 Besançon, France*

(Received 25 July 2017; revised manuscript received 16 October 2017; published 9 January 2018)

We investigate the optical force exerted on a parity-time-symmetric bilayer made of balanced gain and loss. We show that an *asymmetric* optical pulling or pushing force can be exerted on this system depending on the direction of impinging light. The optical pulling or pushing force has a direct physical link to the optical characteristics embedded in the non-Hermitian bilayer. Furthermore, we suggest taking advantage of the optically generated asymmetric force to launch vibrations of an arbitrary shape, which is useful for the contactless probing of mechanical deformations.

DOI: 10.1103/PhysRevApplied.9.014007

I. INTRODUCTION

In 1998, Bender and Boettcher introduced a parity-time ($\mathcal{PT}$)-symmetric quantum mechanics as an extension of conventional quantum mechanics into the complex domain [1,2]. $\mathcal{PT}$-symmetric quantum mechanics was initially an interesting mathematical discovery [3], but it has since been studied in many areas of physics [4–14].

In principal, a quantum system with a non-Hermitian Hamiltonian is $\mathcal{PT}$ symmetric if the Hamiltonian is invariant under combined parity inversion and time reversal. In optics, $\mathcal{PT}$-symmetric systems can be obtained with *balanced* gain and loss and should satisfy $n(\mathbf{r}) = n^*(-\mathbf{r})$ [7]. In other words, the real part of the refractive index is an even function and the imaginary part of the refractive index an odd function of the space. Indeed, once gains and losses are introduced in the problem, the Hamiltonian of such systems becomes non-Hermitian. In general, the eigenvalues of such a system can be real or complex. For real eigenvalues, the $\mathcal{PT}$ symmetry of the system is unbroken (i.e., the system is in a *$\mathcal{PT}$-symmetric phase*), whereas, for complex eigenvalues, the $\mathcal{PT}$ symmetry of the system is broken (i.e., the system is in a *broken $\mathcal{PT}$-symmetric phase*). The concept of $\mathcal{PT}$ symmetry has been used in numerous applications, such as extraordinary nonlinear behaviors [6], asymmetric propagation [8], unidirectional invisibility [9], optical lasing [11], optical switching [15], and many others. However, the physics of the optical force on $\mathcal{PT}$-symmetric systems has *not* yet been fully explored.

It is well known that a highly collimated light beam exerts a *pushing* force (i.e., in the direction of the flow of light) on an arbitrary object [16,17]. However, the direction of the exerted optical force can be changed by using impinging sources of various angles or using an object with different material properties (i.e., permittivity and permeability). For example, one can obtain a counterintuitive force known as the optical *pulling* force [18–26]. It has been shown that a pulling force can be achieved for particular beams, e.g., interference of multiple beams [20] or nonparaxial gradientless beams [21]. An alternative approach makes use of gain materials [18,19]. In all of these approaches, symmetric systems (invariant under space inversion) were investigated, and the system exhibited symmetric optical (pulling and pushing) forces as a result. Consequently, we raise the question as to whether one is able to engineer an *asymmetric optical pulling or pushing* force. In this paper, we address this question by exploring the optical force exerted on one-dimensional $\mathcal{PT}$-symmetric structures. We start by investigating a passive dielectric slab (made of lossy or lossless material, i.e., $n'' \geq 0$, where the refractive index is defined as $n = n' + in''$). We show that the exerted optical force is positive, whereas, for an active slab (made of gain media, i.e., $n'' < 0$), the force sign can change depending on the thickness and the refractive index of the slab. Balancing gain and loss in the context of $\mathcal{PT}$ symmetry provides an alternative route to unveil non-Hermitian optical forces in such a layered structure. To understand the underlying physics of optical pulling and pushing forces in $\mathcal{PT}$-symmetric structures, we calculate the eigenvalues and modulate the $\mathcal{PT}$ phase-transition parameters. We find that the exerted force on a bilayer system changes from pushing to pulling at the $\mathcal{PT}$ exceptional point. Finally, we explain how such a bilayer $\mathcal{PT}$-symmetric structure can be utilized to generate waves in thin elastic layers. Note that having

*Corresponding author.
rasoul.alaee@mpl.mpg.de

losses in metals and dielectrics are commonly used in the Lorentz model; gain is less obvious but mainly explored in the semiconductor field—and especially in quantum dots [27,28]. It is important to mention that designing a specific gain value is not a trivial step. However, several $\mathcal{PT}$-symmetric systems have been experimentally observed in optics [29–32].

II. THEORY

The system shown in Fig. 1(a) is a bilayer made of individual gain and loss layers fulfilling the $\mathcal{PT}$-symmetry condition $n(\mathbf{r}) = n^*(-\mathbf{r})$. The associated incoming (a_1, a_2) and outgoing (b_1, b_2) wave amplitudes are depicted in Fig. 1(a) and can be related by the transfer matrix

$$\begin{pmatrix} b_2 \\ a_2 \end{pmatrix} = \mathbf{M}\begin{pmatrix} a_1 \\ b_1 \end{pmatrix} = \begin{pmatrix} M_{11} & M_{12} \\ M_{21} & M_{22} \end{pmatrix}\begin{pmatrix} a_1 \\ b_1 \end{pmatrix}, \quad (1)$$

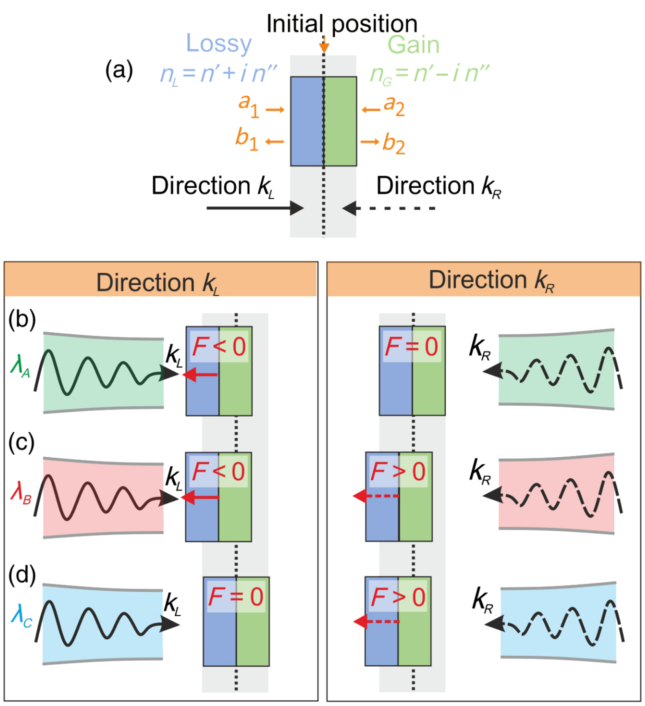

FIG. 1. Principle of a $\mathcal{PT}$ bilayer made of gain (green) and loss (blue) media. (a) The bilayer can be illuminated from the left or the right side. The a_i and b_j define the *incoming* and *outgoing* direction, respectively, for the S-matrix formalism. We illustrate a few possible responses of the system under k_L (from left) and k_R (from right) illumination at different wavelengths λ_i (detailed in Fig. 4). (b) The bilayer illuminated from the left, k_L at λ_A, induces a negative force on the overall system and pulls the bilayer. (For k_R, the overall force in null.) (c) An illumination from the left is selected at another wavelength, λ_B, such that the overall force pulls the bilayer for k_L and pushes it for k_R. (d) An illumination from the left is selected at yet-another wavelength, λ_C, such that the overall force is zero for k_L, whereas the light pushes the bilayer for k_R.

For a $\mathcal{PT}$-symmetric structure, the components of the $\mathbf{M}$ matrix should obey the following properties: $M_{11} = M_{22}^*$ and $\mathrm{Re}[M_{12}] = \mathrm{Re}[M_{21}] = 0$ [8].

From $\mathbf{M}$, the reflection and transmission coefficients can be obtained: $t_L = \det(M)/M_{22}$, $t_R = 1/M_{22}$, $r_R = M_{12}/M_{22}$, and $r_L = -M_{21}/M_{22}$. It is important to mention that, for a reciprocal system, $t = t_R = t_L$ and $\det(M) = 1$ [33]. Thus, the transfer $\mathbf{M}$ and scattering $\mathbf{S}$ matrices can be written as

$$\mathbf{M} = \begin{pmatrix} 1/t^* & r_R/t \\ -r_L/t & 1/t \end{pmatrix}, \qquad \mathbf{S} = \begin{pmatrix} t & r_L \\ r_R & t \end{pmatrix}. \quad (2)$$

For a bilayer, the components of the transfer matrix read [34]

$$M_{11} = (\bar{A} + i\bar{B})e^{-2ik_0 d}, \qquad M_{12} = \bar{C} + i\bar{D},$$
$$M_{21} = \bar{C} - i\bar{D}, \qquad M_{22} = (\bar{A} - i\bar{B})e^{2ik_0 d}, \quad (3)$$

with $\bar{A}$, $\bar{B}$, $\bar{C}$, and $\bar{D}$ defined as

$$\bar{A} = \frac{n_+^2 \cos\psi_+ - n_-^2 \cos\psi_-}{n_+^2 - n_-^2},$$
$$\bar{B} = \frac{\bar{n}_+ n_+ \sin\psi_+ + \bar{n}_- n_- \sin\psi_-}{n_+^2 - n_-^2},$$
$$\bar{C} = \frac{n_- n_+ (\cos\psi_+ - \cos\psi_-)}{n_+^2 - n_-^2},$$
$$\bar{D} = \frac{\bar{n}_+ n_- \sin\psi_- + \bar{n}_- n_+ \sin\psi_+}{n_+^2 - n_-^2}, \quad (4)$$

where $n_\pm = n_L \pm n_G$, $\psi_\pm = n_\pm k_0 d$, $\bar{n}_\pm = n_L n_G \pm 1$, and $n_L = n' + in'' = n_G^*$ is the refractive index of the loss layer.

For a $\mathcal{PT}$-symmetric system, it is easy to show that [35]

$$|T - 1| = \sqrt{R_R R_L}. \quad (5)$$

This relation is known as the generalized unitarity relation, where $T = |t|^2$ is the transmittance, whereas $R_R = |r_R|^2$ and $R_L = |r_L|^2$ are the reflectances for impinging light from the right and the left, respectively.

The time-averaged optical force [36] exerted on a system contained in a closed surface S is given by

$$\mathbf{F} = \oint_S \langle \bar{\bar{\mathbf{T}}} \rangle \cdot \mathbf{n}\, dS, \quad (6)$$

where S is a surface enclosing the slab, $\mathbf{n}$ is normal to S, and $\bar{\bar{\mathbf{T}}}$ is the time-averaged Maxwell stress tensor that is defined as [36]

$$\langle \bar{\bar{\mathbf{T}}} \rangle = \frac{1}{2}\mathrm{Re}\left[\epsilon_0 \mathbf{E}\mathbf{E}^* + \mu_0 \mathbf{H}\mathbf{H}^* - \frac{1}{2}(\epsilon_0 \mathbf{E}\cdot\mathbf{E}^* + \mu_0 \mathbf{H}\cdot\mathbf{H}^*)\mathbf{I}\right], \quad (7)$$

with $\mathbf{E}$ and $\mathbf{H}$ being the complex total electric and magnetic fields, and $\mathbf{I}$ the identity matrix. Note that $\mathbf{E}\cdot\mathbf{E}^*$ and $\mathbf{E}\mathbf{E}^*$

are dot and tensor products, respectively. It can be shown (see the Appendix) that the optical force *per unit surface area* exerted on the slab by a linearly polarized plane wave at normal incidence propagating in the $\mathbf{e}_k$ direction is given by

$$\mathbf{F} = \frac{I_0}{c}(1 + R - T)\mathbf{e}_k. \tag{8}$$

It is important to note that this relation can also be understood from the change of linear momentum, where $(I_0/c)\mathbf{e}_k$ is the incident momentum, $-(I_0/c)R\mathbf{e}_k$ is the reflected momentum and $(I_0/c)T\mathbf{e}_k$ is the transmitted momentum [16,37]. We begin by investigating the optical force generated by a linearly polarized plane wave on a slab made of either passive or gain media. For simplicity, we restrict ourselves to normal-incidence radiation.

In general, for a slab made of passive materials, i.e., $n'' \geq 0$, the reflection, transmission, and absorption are non-negative. Therefore, by using Eq. (8) and $A = 1 - R - T$, $F = I_0/c(2R + A)$, we can conclude that the optical force should be non-negative, $F \geq 0$ [see Figs. 2(a), 2(b), and 2(c)]. The maximum optical force $F_{\max} = 2I_0/c$ can be obtained for a perfect mirror, i.e., $R = 1$, which is twice the force exerted by a perfectly absorbing layer, i.e., $A = 1$. In Fig. 2(c), it can be seen that the force is converging to a positive value, i.e., $I_0/c(1 + R)$ $(T \approx 0)$ for a very thick layer, i.e., $n'd/\lambda \gg 1$. Interestingly, zero optical force can be achieved for a lossless slab ($n'' = 0$) when the slab is transparent, i.e., $R = 0$, $T = 1$. This zero optical force occurs when $d = m\lambda/2n'$ [see Fig. 2(b)], where m is a positive integer.

For a slab made of gain material, the exerted force can be negative, i.e., pulling [see Figs. 2(a) and 2(d)]. The important aspect of this simple configuration is that the layer supports Fabry-Perot resonances and gives rise to multiple interesting points where the force changes sign as a function of the thickness or wavelength, i.e., d/λ. These resonances coincide with the resonances that are observed in the lossless case (these Fabry-Perot resonances occur at $d = m\lambda/2n'$). These results are similar to those reported in other studies [19,23].

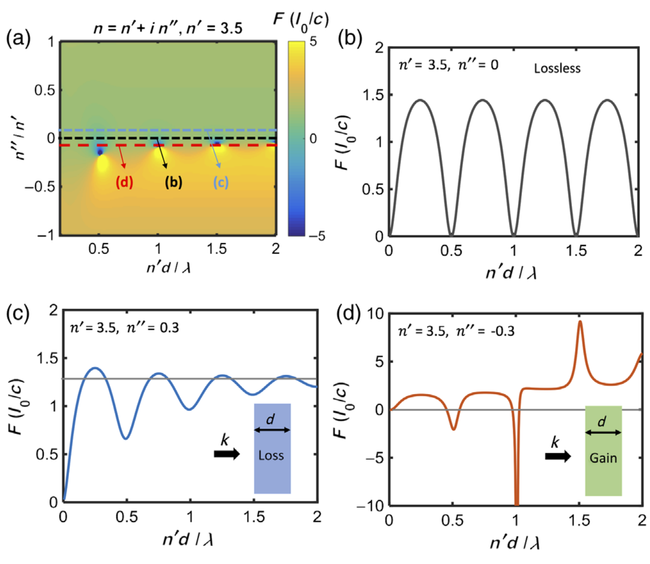

FIG. 2. Optical force exerted on a single slab made of a gain or a lossy material. (a) Normalized optical force exerted on a slab as a function of the refractive-index ratio, i.e., (n''/n'), and the thickness of the dielectric layer, d. We depict as a one-dimensional plot a few selected regions of (a) in the following. (b)–(d) Normalized optical force exerted on a single slab as a function of thickness: (b) lossless, i.e., $n'' = 0$, (c) lossy, i.e., $n'' = 0.3$, (d) gain, i.e., $n'' = -0.3$.

We now assemble a bilayer made of a balanced gain and loss to study the $\mathcal{PT}$-symmetric case. We plot the force exerted on such a slab from different directions, as illustrated in Figs. 1(a) (from the left) and 1(b) (from the right). The solid line represents illumination coming in from the left (see Fig. 1), whereas the dashed line represents the case for right illumination. First, it can be clearly seen that the exerted forces are *not* symmetric for the two opposing irradiation directions (see Fig. 3). The asymmetric forces can be understood from the fact that the system is *not* invariant under space inversion [38,39]. We use the well-known $\mathcal{PT}$ phase-transition parameters, i.e., $n'd/\lambda$ and n''/n' [35,40–42], to conduct a detailed study concerning their influence on the optical forces, transmission, and eigenvalues of the scattering matrix:

$$s_{1,2} = t \pm \sqrt{r_L r_R}, \tag{9}$$

Using $r_L r_R = t^2(1 - 1/T)$ [35], the eigenvalues can be also written as

$$s_{1,2} = t(1 \pm \sqrt{1 - 1/T}). \tag{10}$$

Furthermore, we discuss how these quantities are interrelated with growing loss and gain and also the wavelength.

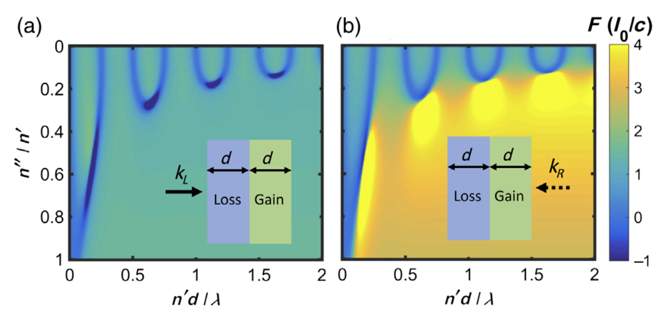

FIG. 3. Optical force exerted on a one-dimensional $\mathcal{PT}$-symmetric structure. (a),(b) Normalized optical force exerted on a bilayer made of balanced gain and loss as a function of the refractive-index ratio, i.e., (n''/n'), and thickness of the dielectric layers for forward (k_L) and backward (k_R) plane-wave illuminations, respectively. The yellow and blue (in the color bar) correspond to the pushing and pulling forces, respectively.

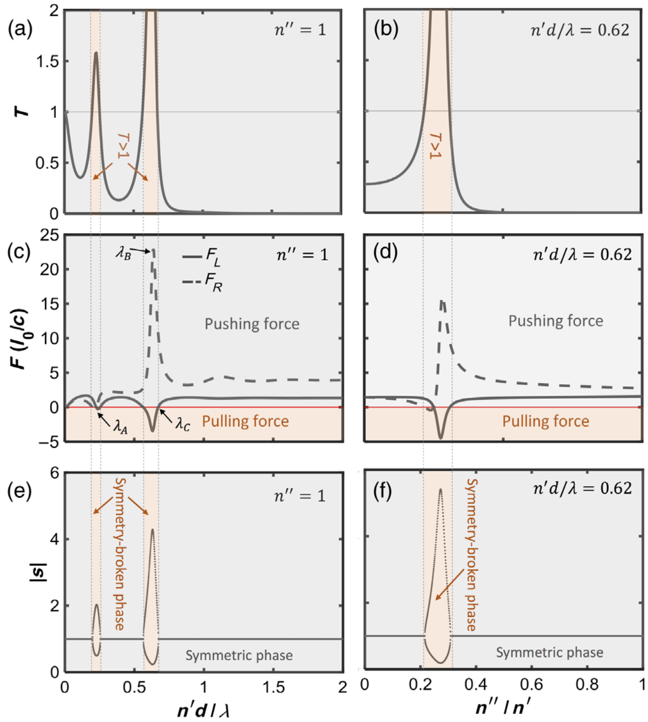

FIG. 4. Optical force exerted on a one-dimensional $\mathcal{PT}$-symmetric structure. (a),(b) Transmission spectra as a function of the normalized dielectric spacer, i.e., $n'd/\lambda$, and the refractive-index ratio, i.e., (n''/n'), respectively. (c),(d) Normalized optical force exerted on a bilayer as a function of the refractive-index ratio, i.e., (n''/n'), and the thickness of the dielectric spacer for both illumination directions, respectively. (e),(f) The modulus of the eigenvalues of the S matrix. The yellow and gray shadows show the symmetry-broken and symmetric phases, respectively.

As computed in Fig. 4, we are able to trace the behavior of the computed optical forces acting on the $\mathcal{PT}$-symmetric bilayer according to their immediate phases.

A. Symmetric phase

The symmetric phase is characterized by unimodular eigenvalues $|s_{1,2}| = 1$, where the transmission remains $T < 1$, as seen in Figs. 4(a)–4(f). By using Eq. (5), the transmission can be obtained from $T = 1 - \sqrt{R_R R_L}$, and the forces are expressed as $F_{R,L} = (I_0/c)(R_{R,L} + \sqrt{R_R R_L})$. In the case of $R_R = R_L$, the forces will be identical for both directions, i.e., $F_R = F_L$. Most importantly, in this phase, the forces are pushing (being positive) for both illumination directions.

B. Exceptional point

The exceptional point occurs at unity transmission $T = 1$ and marks the onset of broken symmetry. Using Eq. (5), it can be easily seen that one of the reflectances vanishes. According to the optical mode profile at the exceptional point that leads to unidirectional reflection, light irradiating the lossy layer is perfectly absorbed, which gives rise to a one-way optical pushing force, i.e., $F_R = (I_0/c)R_R$ and $F_L = 0$; see Figs. 4(c) and 4(d). Here, we obtain an *optical-force rectifier*. An important question one might ask is, what is happening to the force when we approach the exceptional point? Can we get some practical instabilities and undesired effects? In fact, no. It is clear from Figs. 4(c) and 4(d) that the force modulus is continually changing from positive to negative value passing by zero. Thus, this change in the sign of the force is not a problem in practice, as this full region instead exhibits no force. Alternatively, by tuning the pump source of the gain media, we can expect oscillation and even use them in a smart way.

C. Broken-symmetry phase

The broken-symmetry phase is accompanied with larger-than-unity transmission $T > 1$. In this phase, we obtain coexisting amplifying $|s_1| > 1$ and attenuating $|s_2| < 1$ eigenvalues; see Figs. 4(e) and 4(f). Using Eqs. (5) and (8), the force is $F_{R,L} = (I_0/c)(R_{R,L} - \sqrt{R_R R_L})$. It is obvious that if $R_R = R_L$, the force is zero in both directions, i.e., $F_R = F_L = 0$. Interestingly, the coexistence of optical amplification and attenuation within the broken phase produces opposite pushing and pulling forces when illuminated from their respective directions, as we depict in Figs. 4(c) and 4(d).

Next we study the formation of the exceptional point by discussing whether its onset stems solely from optical properties or if it can be controlled by increasing the layering numbers. We discuss two cases: (a) a single bilayer ($N = 1$) and (b) a finite array with $N = 10$. Using the Chebyshev identity, the transfer matrix for N bilayers can be written [43–45]

$$\mathbf{M}_N = \begin{pmatrix} \frac{1}{t^*}\frac{\sin(N\phi)}{\sin\phi} - \frac{\sin[(N-1)\phi]}{\sin\phi} & \frac{r_R}{t}\frac{\sin(N\phi)}{\sin\phi} \\ -\frac{r_L}{t}\frac{\sin(N\phi)}{\sin\phi} & \frac{1}{t}\frac{\sin(N\phi)}{\sin\phi} - \frac{\sin[(N-1)\phi]}{\sin\phi} \end{pmatrix}, \qquad (11)$$

where $\cos\phi = \mathrm{Re}(1/t)$. The total transmission for N bilayers reads [44,45]

$$\frac{1}{T_N} = 1 + \left(\frac{1}{T} - 1\right)\frac{\sin^2(N\phi)}{\sin^2\phi}. \qquad (12)$$

For N bilayers, the eigenvalues of the scattering matrix are $s_{1,2}^N = t_N(1 \pm \sqrt{1 - 1/T_N})$, where t_N and $T_N = |t_N|^2$ are the transmission coefficient and the transmittance, respectively. It can be shown that the eigenvalues of N bilayers can be written as

$$s_{1,2}^N = t_N\left[1 \pm \sqrt{\left(1 - \frac{1}{T}\right)\frac{\sin^2(N\phi)}{\sin^2\phi}}\right]. \qquad (13)$$

Therefore, the exceptional point of the N bilayers occurs when $T = 1$, which is identical to the exceptional point of

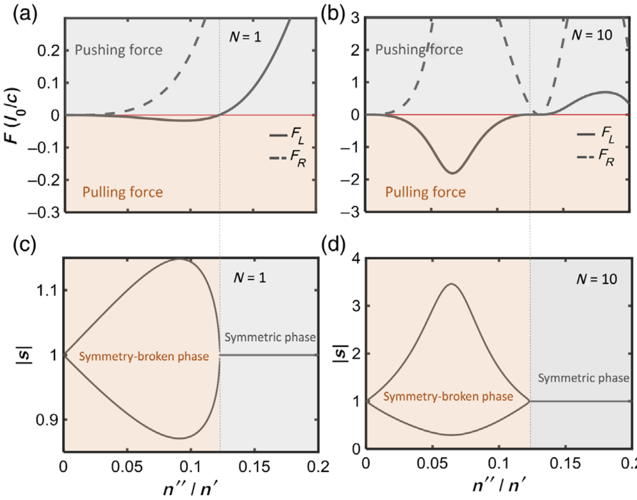

FIG. 5. Optical force exerted on a one-dimensional $\mathcal{PT}$-symmetric structure made of N bilayers. (a),(b) Normalized optical force exerted on a bilayer as a function of the refractive-index ratio, i.e., (n''/n'), and the thickness of the dielectric space for forward and backward plane-wave illuminations, respectively. (c),(d) The modulus of the eigenvalues of the S matrix. The yellow and gray shadows show the symmetry-broken and symmetric phases, respectively. The thickness of each layer is $d = 0.75\lambda/n'$.

a single bilayer. We show the computation of the force as well as the eigenvalues of the scattering matrix in Fig. 5. We can clearly see that, for one or ten bilayers, the exceptional point is the same. We can then conclude that the exceptional point (EP) is a direct property of the bilayer alone, like the Hamiltonian for a closed system. It is then sufficient to look at a single bilayer's EP in order to determine the symmetric and broken-symmetric phase region of any structure made of such bilayers.

Owing to the ability to push and pull a non-Hermitian object from the same side enables one to optically engineer mechanical deflections in bilayers almost entirely at will. By designing a bilayer with a specific thickness and the $\mathcal{PT}$ phase-transition parameters, we propose a mechanical wave generator when different sections, as illustrated in Fig. 6(a), are illuminated at specific wavelengths to ensure the desired optomechanical response. Using a number of wavelength-specific lasers along the bilayer, under static illumination, one is able to preconstrain a large bilayer slab. In Figs. 6(b) and 6(c), we illustrate three specific examples of how one can generate preconstrained deformations on a thin plate. Once released, the preconstrained part generates a wave propagating parallel to the slab. If the slab is thin (compare to the wavelength), one can generate a flexural-like wave. This would be a contactless and quick way of setting the wave shape on a thin layer (see Fig. 6). Conceptually, to get the right deformation, one can assume that the optical force is a constant force in respect to the mechanical dynamics. We consider that, at a given time, one can have all of the required pulling and pushing lasers

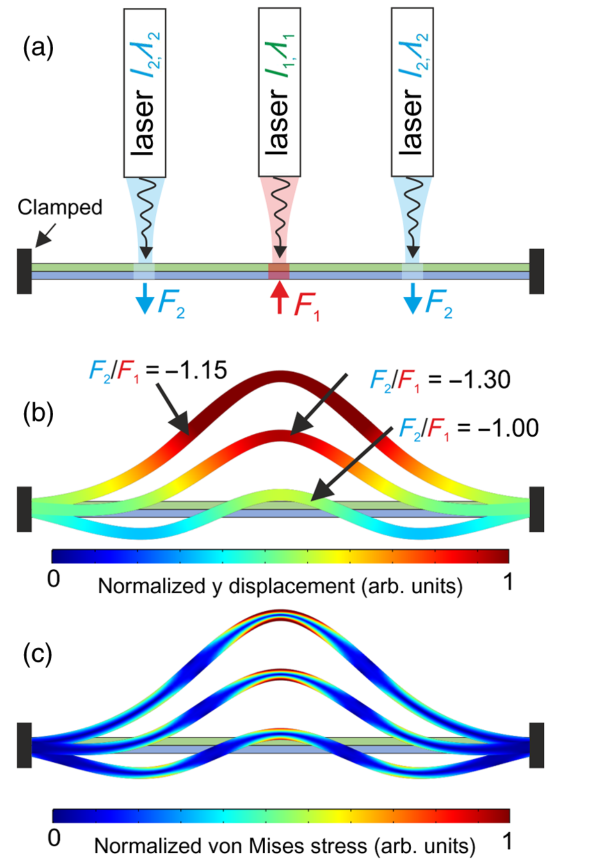

FIG. 6. Principle of a mechanical wave generator using $\mathcal{PT}$-symmetric media. As illustrated in Figs. 1 and 4, for different wavelengths, one can get a pulling or pushing behavior. Combining two lasers with different wavelengths (λ_i) and intensities (I_i), one can get at the same time a local deformation of a thin layer that is due to the local pulling or pushing. We simply have to select two working regions such that the overall force can be positive or negative. The amplitude of the force F_i is dependent on the laser amplitude, i.e., it can be selected such that one can get the desired ratio and sign of F_2/F_1. (b) Different induced prestrained cases of F_2/F_1. (c) The deformed geometry shown with the von Mises stress induced inside. All values are normalized. This shapes the prestressed state of the layer. Once the laser is turned off, the prestress can generate a wave packet. Red arrows indicate the direction of the local force exerted by the laser.

on. Optical dynamics being much faster than the mechanical one, we can almost consider the extent of the laser with the illuminated areas to be subject to a constant force. This force is controllable by the user and can be tuned at wish. Finding the equilibrium position of a plate clamped on the outer boundaries and under a stress field is then trivial from a numerical point of view. Obviously, we obtain the schematics of Fig. 6 under these considerations.

III. CONCLUSIONS

In conclusion, we have theoretically demonstrated that a highly collimated laser (a single plane wave) can exert an asymmetric pulling or pushing force on a $\mathcal{PT}$-symmetric optical layer. The physics of the optical pulling or pushing force is fully explained in the context of $\mathcal{PT}$ symmetry and the exceptional point. This mechanical behavior can be used to generate elastic waves in thin layers.

ACKNOWLEDGMENTS

We thank V. Laude, B. Gürlek, D.-M. Cano, Y. Achaoui, M. Wegener, and V. Sandoghdar for the constructive discussions and their suggestions. R. A. would like to acknowledge financial support from the Max Planck Society. J. C. acknowledges the support from the European Research Council (ERC) through Starting Grant No. 714577 PHONOMETA and from Ministerio de Economía, Industria y Competitividad (MINECO) through a Ramón y Cajal grant (Grant No. RYC-2015-17156). This project was performed in cooperation with the Labex ACTION program (Contract No. ANR-11-LABX-0001-01), and this work was supported by the French "Investissements d'Avenir" program, project ISITE-BFC (Contract No. ANR-15-IDEX-03).

APPENDIX: OPTICAL FORCES EXERTED ON A DIELECTRIC SLAB

In this appendix, we derive an expression for optical force exerted by a plane wave on a dielectric slab. Let us consider that the slab is illuminated by a linearly polarized plane wave propagating along the z axis at normal incidence, i.e., $\mathbf{E}_i = E_0 e^{ikz}\mathbf{e}_x$ (see Fig. 7). The reflected and transmitted electric fields can be written as

$$\mathbf{E}_r = E_r e^{ikz}\mathbf{e}_x, \qquad \mathbf{E}_t = E_t e^{ikz}\mathbf{e}_x,$$

and the magnetic fields can be obtained as $\mathbf{H} = (1/kZ_0)(\mathbf{k}\times\mathbf{E})$, where Z_0 is the impedance of the free

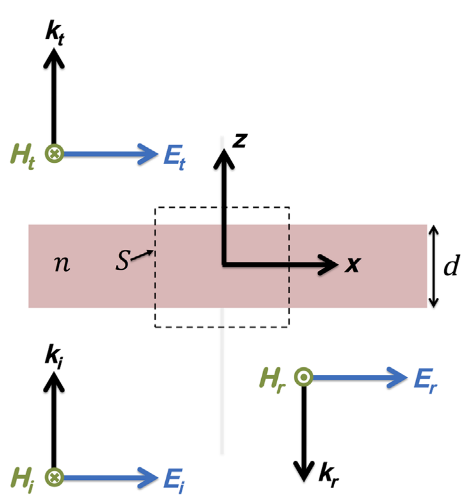

FIG. 7. Schematic view of a dielectric slab of thickness d with refractive index n illuminated with a linearly polarized plane wave. The reflected and transmitted electric and magnetic fields are depicted. The dashed box shows the closed surface for integrating the Maxwell stress tensor.

space. The Maxwell stress tensor at $z > d/2$ can be calculated by using the total electric and magnetic fields, i.e., $\mathbf{E} = E_t e^{ikz}\mathbf{e}_x$, $\mathbf{H} = H_t e^{ikz}\mathbf{e}_y$:

$$\begin{aligned}\langle \overline{\overline{\mathbf{T}}}\rangle_{z>d/2} &= \frac{1}{2}\epsilon_0|E_t|^2\mathbf{e}_x\mathbf{e}_x + \frac{1}{2}\mu_0|H_t|^2\mathbf{e}_y\mathbf{e}_y \\ &\quad -\frac{1}{4}[\epsilon_0|E_t|^2+\mu_0|H_t|^2]\mathbf{e}_z\mathbf{e}_z. \end{aligned} \tag{A1}$$

Similarly, by using the total electric and magnetic fields at $z < -d/2$, i.e., $\mathbf{E} = (E_i e^{ikz} + E_r e^{-ikz})\mathbf{e}_x$, $\mathbf{H} = (H_i e^{ikz} - H_t e^{-ikz})\mathbf{e}_y$, the corresponding Maxwell stress tensor reads

$$\begin{aligned}\langle \overline{\overline{\mathbf{T}}}\rangle_{z<-d/2} &= \frac{1}{2}\epsilon_0|E_i e^{ikz} + E_r e^{-ikz}|^2\mathbf{e}_x\mathbf{e}_x \\ &\quad +\frac{1}{2}\mu_0|H_i e^{ikz} - H_r e^{-ikz}|^2\mathbf{e}_y\mathbf{e}_y \\ &\quad -\frac{1}{4}[\epsilon_0|E_i e^{ikz} + E_r e^{-ikz}|^2 \\ &\quad +\mu_0|H_i e^{ikz} - H_r e^{-ikz}|^2]\mathbf{e}_z\mathbf{e}_z. \end{aligned} \tag{A2}$$

Finally, the optical force derived by integrating the Maxwell stress tensor on a close surface S can be written as

$$\begin{aligned}\mathbf{F} &= \oint_S \langle \overline{\overline{\mathbf{T}}}\rangle \cdot \mathbf{n}da, \\ &= A_s(-\langle \overline{\overline{\mathbf{T}}}\rangle_{z<-d/2}\cdot\mathbf{e}_z + \langle \overline{\overline{\mathbf{T}}}\rangle_{z>d/2}\cdot\mathbf{e}_z), \\ &= \frac{1}{2}\epsilon_0 A_s(|E_0|^2 + |E_r|^2 - |E_t|^2)\mathbf{e}_z, \\ &= \frac{I_0}{c}A_s[1+|r|^2-|t|^2]\mathbf{e}_z, \end{aligned} \tag{A3}$$

where r and t are the reflection and transmission coefficients, respectively. $I_0 = \frac{1}{2}\epsilon_0 c|E_0|^2$ is the intensity of the incident plane wave, while A_s is the area. A similar expression for the optical force can be obtained by using the Lorentz force acting on both currents $\mathbf{J}$ due to the polarization of the dielectric slab and the bound charges ρ_e at the boundaries, i.e.,

$$\mathbf{F} = \frac{1}{2}\mathrm{Re}\left[\int_V \langle \rho_e\mathbf{E}^* + \mathbf{J}\times\mathbf{B}^*\rangle dV\right]. \tag{A4}$$

The derivation of the optical force exerted on the slab using the Lorentz force can be found in Refs. [16,37].

[1] Carl M. Bender and Stefan Boettcher, Real Spectra in Non-Hermitian Hamiltonians Having $\mathcal{PT}$ Symmetry, Phys. Rev. Lett. 80, 5243 (1998).

[2] Carl M. Bender, Dorje C. Brody, and Hugh F. Jones, Complex Extension of Quantum Mechanics, Phys. Rev. Lett. **89**, 270401 (2002).

[3] Carl M. Bender, $\mathcal{PT}$ symmetry in quantum physics: From a mathematical curiosity to optical experiments, Europhys. News **47**, 17 (2016).

[4] Graeme Milton, *Extending the Theory of Composites to Other Areas of Science* (Milton & Patton Publishing, Salt Lake City, 2016).

[5] Graeme Milton and Ornella Mattei, Field patterns: A new mathematical object, Proc. R. Soc. A **473**, 20160819 (2017).

[6] Z. H. Musslimani, K. G. Makris, R. El-Ganainy, and D. N. Christodoulides, Optical Solitons in $\mathcal{PT}$ Periodic Potentials, Phys. Rev. Lett. **100**, 030402 (2008).

[7] R. El-Ganainy, K. G. Makris, D. N. Christodoulides, and Ziad H. Musslimani, Theory of coupled optical $\mathcal{PT}$-symmetric structures, Opt. Lett. **32**, 2632 (2007).

[8] Stefano Longhi, $\mathcal{PT}$-symmetric laser absorber, Phys. Rev. A **82**, 031801 (2010).

[9] Zin Lin, Hamidreza Ramezani, Toni Eichelkraut, Tsampikos Kottos, Hui Cao, and Demetrios N. Christodoulides, Unidirectional Invisibility Induced by $\mathcal{PT}$-Symmetric Periodic Structures, Phys. Rev. Lett. **106**, 213901 (2011).

[10] Richard V. Craster and Sébastien Guenneau, *Acoustic Metamaterials: Negative Refraction, Imaging, Lensing and Cloaking* (Springer Science+Business Media, New York, 2012).

[11] Hossein Hodaei, Mohammad-Ali Miri, Matthias Heinrich, Demetrios N. Christodoulides, and Mercedeh Khajavikhan, Parity-time–symmetric microring lasers, Science **346**, 975 (2014).

[12] R. Fleury, D. Sounas, and A Alu, An invisible acoustic sensor based on parity-time symmetry, Nat. Commun. **6**, 5905 (2014).

[13] J. Christensen, M. Willatzen, V. R. Velasco, and M.-H. Lu, Parity-Time Synthetic Phononic Media, Phys. Rev. Lett. **116**, 207601 (2016).

[14] Yves Aurégan and Vincent Pagneux, $\mathcal{PT}$, Phys. Rev. Lett. **118**, 174301 (2017).

[15] Anatole Lupu, Henri Benisty, and Aloyse Degiron, Using optical $\mathcal{PT}$-symmetry for switching applications, Photonics Nanostruct. Fundam. Appl. **12**, 305 (2014).

[16] Masud Mansuripur, *Field, Force, Energy and Momentum in Classical Electrodynamics* (Bentham Science Publishers, Sharjah, United Arab Emirates, 2011).

[17] Aso Rahimzadegan, Rasoul Alaee, Ivan Fernandez-Corbaton, and Carsten Rockstuhl, Fundamental limits of optical force and torque, Phys. Rev. B **95**, 035106 (2017).

[18] S. Sukhov and A. Dogariu, On the concept of tractor beams, Opt. Lett. **35**, 3847 (2010).

[19] Amit Mizrahi and Yeshaiahu Fainman, Negative radiation pressure on gain medium structures, Opt. Lett. **35**, 3405 (2010).

[20] Jun Chen, Jack Ng, Zhifang Lin, and C. T. Chan, Optical pulling force, Nat. Photonics **5**, 531 (2011).

[21] Andrey Novitsky, Cheng-Wei Qiu, and Haifeng Wang, Single Gradientless Light Beam Drags Particles as Tractor Beams, Phys. Rev. Lett. **107**, 203601 (2011).

[22] Juan Jose Saenz, Optical forces: Laser tractor beams, Nat. Photonics **5**, 514 (2011).

[23] Kevin J. Webb and Shivanand, Negative electromagnetic plane-wave force in gain media, Phys. Rev. E **84**, 057602 (2011).

[24] Aristide Dogariu, Sergey Sukhov, and José Sáenz, Optically induced negative forces, Nat. Photonics **7**, 24 (2013).

[25] David E. Fernandes and Mário G. Silveirinha, Optical tractor beam with chiral light, Phys. Rev. A **91**, 061801 (2015).

[26] David E. Fernandes and Mário G. Silveirinha, Single-Beam Optical Conveyor Belt for Chiral Particles, Phys. Rev. Applied **6**, 014016 (2016).

[27] Kevin J. Webb and Alon Ludwig, Semiconductor quantum dot mixture as a lossless negative dielectric constant optical material, Phys. Rev. B **78**, 153303 (2008).

[28] Koo-Chul Je, In-Chul Shin, Jihoon Kim, and Kwangseuk Kyhm, Optical nonlinearities of fine exciton states in a CdSe quantum dot, Appl. Phys. Lett. **97**, 103110 (2010).

[29] A. Guo, G. J. Salamo, D. Duchesne, R. Morandotti, M. Volatier-Ravat, V. Aimez, G. A. Siviloglou, and D. N. Christodoulides, Observation of $\mathcal{PT}$-Symmetry Breaking in Complex Optical Potentials, Phys. Rev. Lett. **103**, 093902 (2009).

[30] Christian E. Rüter, Konstantinos G. Makris, Ramy El-Ganainy, Demetrios N. Christodoulides, Mordechai Segev, and Detlef Kip, Observation of parity-time symmetry in optics, Nat. Phys. **6**, 192 (2010).

[31] Liang Feng, Ye-Long Xu, William S. Fegadolli, Ming-Hui Lu, José E. B. Oliveira, Vilson R. Almeida, Yan-Feng Chen, and Axel Scherer, Experimental demonstration of a unidirectional reflectionless parity-time metamaterial at optical frequencies, Nat. Mater. **12**, 108 (2013).

[32] Hossein Hodaei, Absar U. Hassan, Steffen Wittek, Hipolito Garcia-Gracia, Ramy El-Ganainy, Demetrios N. Christodoulides, and Mercedeh Khajavikhan, Enhanced sensitivity at higher-order exceptional points, Nature (London) **548**, 187 (2017).

[33] Pochi Yeh, *Optical Waves in Layered Media*, Wiley Series in Pure and Applied Optics Vol. 61 (Wiley InterScience, New York, 2005).

[34] Ali Mostafazadeh, Invisibility and $\mathcal{PT}$ symmetry, Phys. Rev. A **87**, 012103 (2013).

[35] Li Ge, Y. D. Chong, and A. D. Stone, Conservation relations and anisotropic transmission resonances in one-dimensional $\mathcal{PT}$-symmetric photonic heterostructures, Phys. Rev. A **85**, 023802 (2012).

[36] John David Jackson, *Classical Electrodynamics* (Wiley, New York, 1999).

[37] Masud Mansuripur, Radiation pressure and the linear momentum of the electromagnetic field, Opt. Express **12**, 5375 (2004).

[38] R. Alaee, M. Albooyeh, M. Yazdi, N. Komjani, C. Simovski, F. Lederer, and C. Rockstuhl, Magnetoelectric coupling in nonidentical plasmonic nanoparticles: Theory and applications, Phys. Rev. B **91**, 115119 (2015).

[39] Rasoul Alaee, Mohammad Albooyeh, Aso Rahimzadegan, Mohammad S. Mirmoosa, Yuri S. Kivshar, and Carsten Rockstuhl, All-dielectric reciprocal bianisotropic nanoparticles, Phys. Rev. B **92**, 245130 (2015).

[40] Joseph Schindler, Ang Li, Mei C. Zheng, Fred M. Ellis, and Tsampikos Kottos, Experimental study of active *LRC*

circuits with $\mathcal{PT}$ symmetries, Phys. Rev. A **84**, 040101 (2011).

[41] Brian Baum, Hadiseh Alaeian, and Jennifer Dionne, A parity-time symmetric coherent plasmonic absorber-amplifier, J. Appl. Phys. **117**, 063106 (2015).

[42] Mahboobeh Chitsazi, Huanan Li, F. M. Ellis, and Tsampikos Kottos, Experimental Realization of Floquet $\mathcal{PT}$-Symmetric Systems, Phys. Rev. Lett. **119**, 093901 (2017).

[43] Li Ge and Liang Feng, Contrasting eigenvalue and singular-value spectra for lasing and antilasing in a $\mathcal{PT}$-symmetric periodic structure, Phys. Rev. A **95**, 013813 (2017).

[44] V. Achilleos, Y. Aurégan, and V. Pagneux, Scattering by Finite Periodic $\mathcal{PT}$-Symmetric Structures, Phys. Rev. Lett. **119**, 243904 (2017).

[45] D. W. L. Sprung, H. Wu, and J. Martorell, Scattering by a finite periodic potential, Am. J. Phys. **61**, 1118 (1993).